

# Cyclic (Alkyl)(amino)carbene Ligand-Promoted Nitro Deoxygenative Hydroboration with Chromium Catalysis: Scope, Mechanism, and Applications

Lixing Zhao,<sup>§</sup> Chenyang Hu,<sup>§</sup> Xuefeng Cong, Gongda Deng, Liu Leo Liu, Meiming Luo, and Xiaoming Zeng\*

Cite This: *J. Am. Chem. Soc.* 2021, 143, 1618–1629

Read Online

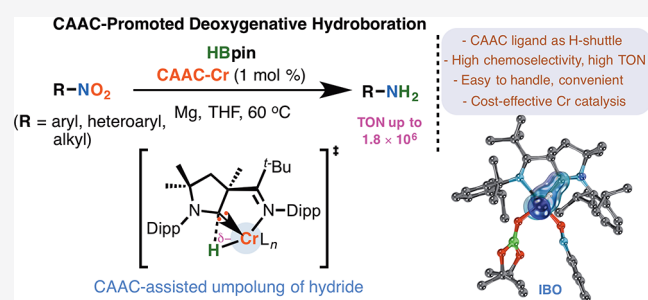
ACCESS |

Metrics & More

Article Recommendations

Supporting Information

**ABSTRACT:** Transition metal catalysis that utilizes *N*-heterocyclic carbenes as noninnocent ligands in promoting transformations has not been well studied. We report here a cyclic (alkyl)(amino)carbene (CAAC) ligand-promoted nitro deoxygenative hydroboration with cost-effective chromium catalysis. Using 1 mol % of CAAC–Cr precatalyst, the addition of HBpin to nitro scaffolds leads to deoxygenation, allowing for the retention of various reducible functionalities and the compatibility of sensitive groups toward hydroboration, thereby providing a mild, chemoselective, and facile strategy to form anilines, as well as heteroaryl and aliphatic amine derivatives, with broad scope and particularly high turnover numbers (up to  $1.8 \times 10^6$ ). Mechanistic studies, based on theoretical calculations, indicate that the CAAC ligand plays an important role in promoting polarity reversal of hydride of HBpin; it serves as an H-shuttle to facilitate deoxygenative hydroboration. The preparation of several commercially available pharmaceuticals by means of this strategy highlights its potential application in medicinal chemistry.



## 1. INTRODUCTION

The prevalence of  $NH_2$  moieties in pharmaceuticals, agrochemicals, dyes, and bulk chemicals has prompted the development of selective strategies for their preparation.<sup>1,2</sup> Convenient routes to prepare  $NH_2$ -bearing anilines and amines have mainly involved the deoxygenation of commercially available nitro motifs, but these routes usually necessitate the use of harsh reductants, such as metal alkali,  $NaBH_4$ , hydrazine, and pressurized  $H_2$ .<sup>3–5</sup> The use of such reactants carries significant safety concerns. Furthermore, their use often leads to the important issue of selectivity, especially when easily reducible functional groups are present in the same molecules (particularly halides, alkynes, and olefins). Hence, easy-to-handle protocols that can be used to deoxygenate nitro motifs mildly and chemoselectively would be a valuable addition to the synthetic toolbox toward amines and anilines.<sup>6–9</sup>

Catalytic hydroboration has emerged as an alternative method to reduce unsaturated compounds and afford valuable chemicals,<sup>10,11</sup> as witnessed by the significant progress made in the hydroboration of unsaturated  $C=O$  bonds in precursors such as ketones,<sup>12–22</sup> aldehydes,<sup>20–22</sup> esters,<sup>23,24</sup> carboxylic acids,<sup>25</sup> and carbon dioxide.<sup>25–28</sup> These reactions commonly afford oxygen-borylated compounds through nucleophilic metal hydride intermediates (Scheme 1a). As far as we are aware, limited success has been achieved in the complete cleavage of oxygen moieties in these precursors, which could

lead to reduction by deoxygenation processes.<sup>29</sup> Deoxygenative hydroboration has been described by Sadow (involving amides)<sup>30</sup> and Findlater (involving lanthanide cluster catalysis)<sup>31</sup> (see Scheme 1b). Marks and Lohr disclosed a robust  $La[N(SiMe_3)_2]_3$  catalyst that efficiently deoxygenates amides, with retention of the unsaturated nitro group.<sup>32</sup>

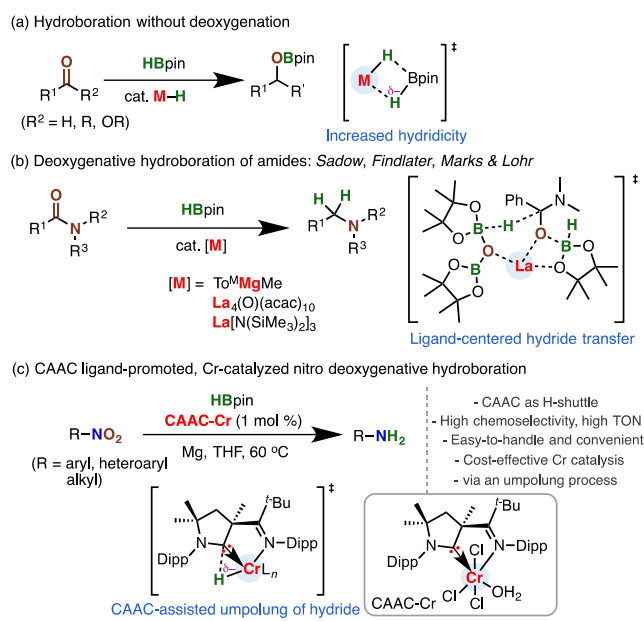
We subsequently questioned whether it is possible to switch the selectivity by preferentially deoxygenating nitro groups while retaining amides and other functionalities sensitive toward hydroboration. However, challenges associated with reversing the polarity of hydride of HBpin for the deoxygenation remain. The umpolung process is therefore required for the formation of  $NH_2$  moieties. Herein, we report a cyclic (alkyl)(amino)carbene (CAAC) ligand-promoted nitro deoxygenative hydroboration reaction, under mild conditions and with cost-effective chromium catalysis, for the convenient formation of  $NH_2$ -containing anilines and amines with 1 mol % catalyst loading (Scheme 1c).<sup>33,34</sup> This reaction favors the

Received: November 25, 2020

Published: January 7, 2021



### Scheme 1. Catalytic Addition of Pinacolborane to Unsaturated Oxygen-Containing Motifs



selective hydroboration of nitro motifs over functional groups of alkynes, alkenes, pyridines, and even amides that are usually hydroborated, through a ligand-assisted umpolung process, using CAAC as an H-shuttle.

## 2. RESULTS AND DISCUSSION

*N*-Heterocyclic carbenes (NHCs) are electron-rich  $\sigma$  donors frequently used as ancillary ligands to bind to metals in the assembly of effective catalysts.<sup>35</sup> As compared to typical NHCs, CAACs show strong nucleophilicity and electrophilicity.<sup>36</sup> They have been utilized to assist metals in promoting hydrofunctionalization, as reported by Bertrand.<sup>37</sup> Considering that electron-rich CAAC ligands are able to enhance the electron density around a Cr center,<sup>37,38</sup> facilitating the activation of the B–H bond by  $\sigma$  interaction, while incorporation of an imino anchor to the side chain of CAAC may stabilize a reactive Cr in catalysis by bidentate coordination, the imino-containing iminium salt **1a** was selected as precursor for the preparation of an organochromium complex (Figure 1).<sup>39</sup> Deprotonation by  $K[N(SiMe_3)_2]$  and treatment with  $CrCl_3$  in THF afforded the CAAC–Cr complex **2a**. X-ray diffraction analysis of the crystal

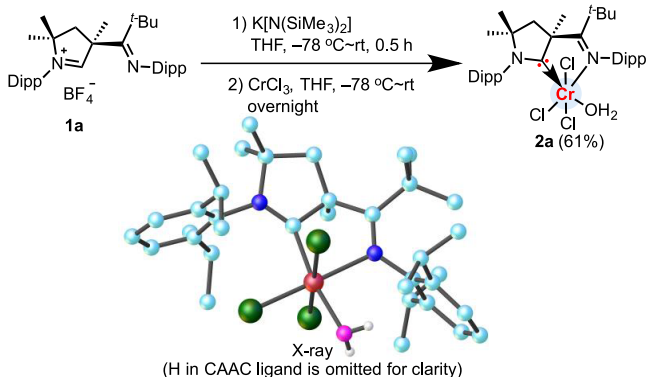


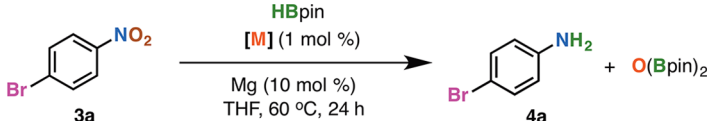
Figure 1. Synthesis of CAAC–Cr complex.

structure revealed that the Cr adopts an octahedral geometry in ligation with CAAC, the imino, and an additional water molecule in the solid state.

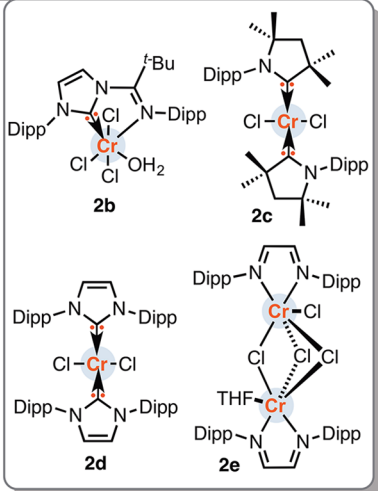
The reactivity of CAAC–Cr complex **2a** in the hydroboration of a nitro group was initially determined in the reaction of 1-bromo-4-nitrobenzene with HBpin (Table 1). It was pleasing to find that the reaction of 1 mol % of **2a** with 10 mol % of Mg as reductant exhibited high reactivity. This reaction allowed the addition of HBpin across a nitro group by a deoxygenation process that proceeded efficiently at 60 °C, leading to reduction and affording the aniline **3a** in 96% yield (entry 1). The deoxygenation tolerates a reducible bromo substituent, without dehalogenation occurring. The formation of bisboryloxide ( $O(Bpin)_2$ ) in nearly quantitative yield was observed.  $O(Bpin)_2$  is a valuable precursor for accessing *n*-type semiconducting polymers,<sup>40</sup> orally active EP3 receptor antagonists,<sup>41</sup> and boryl silyl ethers.<sup>42</sup>

In the absence of a Cr complex, the deoxygenative hydroboration with Mg did not afford an aniline, in recovery of the nitrobenzene. The formation of reactive low-valent Cr by the reduction of **2a** with Mg could be considered for the deoxygenative hydroboration.<sup>43</sup> The replacement of CAAC by the NHC of 1,3-bis(2,6-diisopropylphenyl)imidazol-2-ylidene) in complex **2a** gave an inferior result (**2b**) (entry 2). The CAAC scaffold in the ligand may play an important role in promoting the reactivity of Cr in the deoxygenation of nitro groups. Other complexes, such as CAAC–Cr–CAAC (**2c**), NHC–Cr–NHC (**2d**), and bis(imino)Cr (**2e**), gave relatively low conversions (entries 3–5). Deoxygenation using  $CrCl_3$ ,  $CrCl_2$ , and  $Cr(acac)_3$  gave poor results (entries 6–8). First-row metal salts of  $FeCl_3$ ,  $CoCl_2$ ,  $NiCl_2$ , and  $CuBr_2$ , and  $PdCl_2$  catalyst, exhibited almost no reactivity in the reaction (entries 9–13). Of note is that the CAAC–Cr **2a** exhibited extremely high efficiency; it gave a turnover number (TON) as high as  $1.8 \times 10^6$  in the gram-scale deoxygenative reduction of 4-bromonitrobenzene.

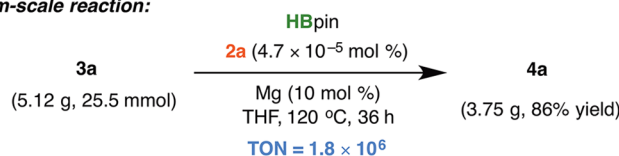
Having in hand the efficient CAAC–Cr complex **2a**, the scope of nitro motifs for the deoxygenative reduction was explored. We proved that the reaction allows for selectively reducing nitro scaffolds while keeping the iodo functionality intact, hence providing access to the substituted aniline **4b** in excellent yield (Scheme 2). The incorporation of a broad range of polar functional groups, including chloro, fluoro, trifluoromethyl, trifluoromethoxy, thiomethyl, pinacol boronate ester, hydroxyl, and amino, has no great influence on the deoxygenative hydroboration. Diversely substituted aniline compounds **4c–m** were formed in yields of 70–99%. Unsaturated alkynes and alkenes are usually sensitive motifs toward hydroboration; they can undergo nucleophilic attack by HBpin under metal and Lewis acid catalysis.<sup>44</sup> Interestingly, the alkyne and olefin scaffolds in nitroarenes are compatible with the reduction system, thereby offering a strategy for the preparation of alkynylated and alkenylated anilines **4n–q**. The primary and secondary amide groups reduced by magnesium, lanthanide, and zinc catalysis can be retained under the present conditions,<sup>30–32,45</sup> affording 4-aminobenzamide (**4r**) and *N*-(4-aminophenyl)benzamide (**4s**). The steric hindrance that resulted from the *ortho*-methyl, -methoxy, and -phenyl substituents did not hamper the deoxygenation (**4u–w**). Through this strategy, benzene-1,2-diamines **4x** and **4y** that contain two of the same, or different, amino scaffolds were successfully derived from the commercially available nitroarene precursors. Difluoro-, dichloro-, bromofluoro-, and amino-

Table 1. Studying the Effect of Complexes on the Deoxygenative Hydroboration of 1-Bromo-4-nitrobenzene<sup>a</sup>


Entry	[M]	Yield (4a)
1	2a	96%
2	2b	78%
3	2c	40%
4	2d	26%
5	2e	53%
6	CrCl <sub>3</sub>	37%
7	CrCl <sub>2</sub>	22%
8	Cr(acac) <sub>3</sub>	20%
9	CoCl <sub>2</sub>	0%
10 <sup>b</sup>	FeCl <sub>3</sub>	5%
11 <sup>b</sup>	NiCl <sub>2</sub>	7%
12	CuBr <sub>2</sub>	0%
13	PdCl <sub>2</sub>	0%



## Gram-scale reaction:



<sup>a</sup>Conditions: 3a (0.5 mmol), metal catalyst (1 mol %), HBpin (2 mmol), Mg (10 mol %) in THF (2 mL), 60 °C, 24 h. <sup>b</sup>Estimated by GC analysis.

chloro-bearing disubstituted anilines were facily accessible in a chemoselective fashion (4z–ac). Considering that groups such as iodide, bromide, alkyne, and alkene are easily dehalogenated or hydrogenated under catalytic hydrogenation,<sup>46</sup> good compatibility of this reaction renders it attractive in the selective formation of anilines containing these valuable functionalities. Nitroarenes containing *O*- and *N*-heterocyclic scaffolds, such as oxazolyl, pyrazolyl, piperidinyl, and morpholinyl, were amenable to the deoxygenative hydroboration, affording functionalized aniline compounds 4af–ai in preparatively useful yields.

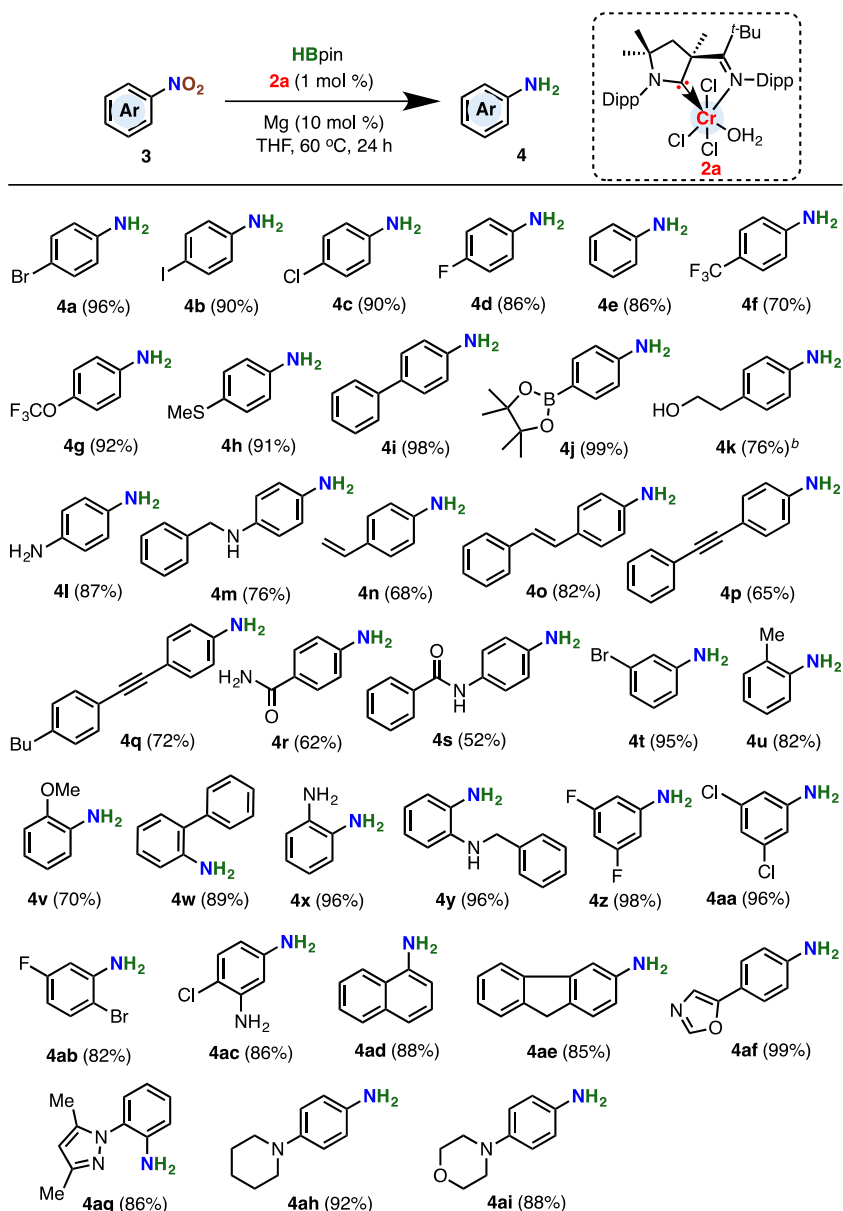
Application of the deoxygenative hydroboration in the synthesis of heteroaromatic amines was then studied. According to the discoveries of Marks, Kinjo, and others, *N*-heteroarenes of pyridines and quinolines react with HBpin by a 1,2- or 1,4-dearomatizative addition to afford *N*-borylated heterocycles.<sup>47–50</sup> We determined that under CAAC–Cr catalysis, only the nitro groups were selectively reduced by deoxygenation, with the *N*-heteroarene intact (Scheme 3). As a result, aminated heterocycles of pyridines and quinolines 6a–g, which serve as core structures frequently found in pharmaceuticals and agrochemicals, were prepared. Furthermore, using this CAAC–Cr-catalyzed system, the nitro scaffolds in a wide range of nitrogen, oxygen, and sulfur heterocycles reacted with HBpin in a smooth manner, thereby offering a strategy to access indolyl, benzo[*b*]thiophenyl, dihydrobenzo[*b*]thiophenyl, dihydrobenzofuranyl, benzo[*d*]-[1,3]dioxolyl, benzo[*d*]thiazolyl, and quinoxalinyll amine compounds 6h–r in good to excellent yields (81–99%).

In an effort to assess the possibility of using this protocol for the preparation of synthetically intriguing aliphatic amine

motifs, nitroalkanes were employed as precursors. The deoxygenative hydroboration of 1-nitrohexane proceeded with 1 mol % of complex 2a at 60 °C to afford the corresponding ammonium derivative 8a in 93% yield, after workup with acid (Scheme 4). Following this protocol, linear aliphatic ammonium derivatives containing butyl, pentanyl, octanyl, 2-methoxyethyl, and 3-methoxypropyl were accessible (8b–f). Interestingly, the incorporation of a hydroxyl into the scaffold of aliphatic hydrocarbons did not shut down the nitro reduction. The hydroxyl-tethered motifs 8k and l were obtained in good yields. The nitro substituents on secondary aliphatic carbons such as isopropane, cyclopropane, cyclopentane, and cyclohexane readily underwent deoxygenation (8m–p).

Further extension of this CAAC–Cr-catalyzed reduction to the synthesis of bulky tertiary ammonium salts bearing *tert*-butyl and 1-adamantyl scaffolds was successful. Substituted aryl and heteroaryl groups in the motifs of nitroalkanes had no effect on the deoxygenation (8s–ac). Functional groups of bromo, chloro, fluoro, methoxy, amino, and pyridyl were retained after the deoxygenation. Interestingly, two nitro substituents in aliphatic hydrocarbons could be synchronously deoxygenated under standard conditions, to afford cyclohexane-1,2-diammonium and octane-1,8-diammonium salts (8ad and ae).

To gain insight into the mechanistic details associated with the CAAC–Cr-catalyzed deoxygenative hydroboration, the kinetic profile was investigated. Here, the reaction of 1-bromo-4-nitrobenzene 3a with HBpin was selected as the model system. Examining the kinetic behavior revealed that the deoxygenative hydroboration proceeds sluggishly to form the

Scheme 2. CAAC–Cr-Catalyzed Chemoselective Deoxygenative Hydroboration of Nitro Arenes<sup>a</sup>

<sup>a</sup>Conditions: nitro compound (0.5 mmol), **2a** (1 mol %), HBpin (2 mmol), Mg (10 mol %) in THF (2 mL), 60 °C, 24 h. Isolated yields are given.

<sup>b</sup>HBpin (5 equiv) was used.

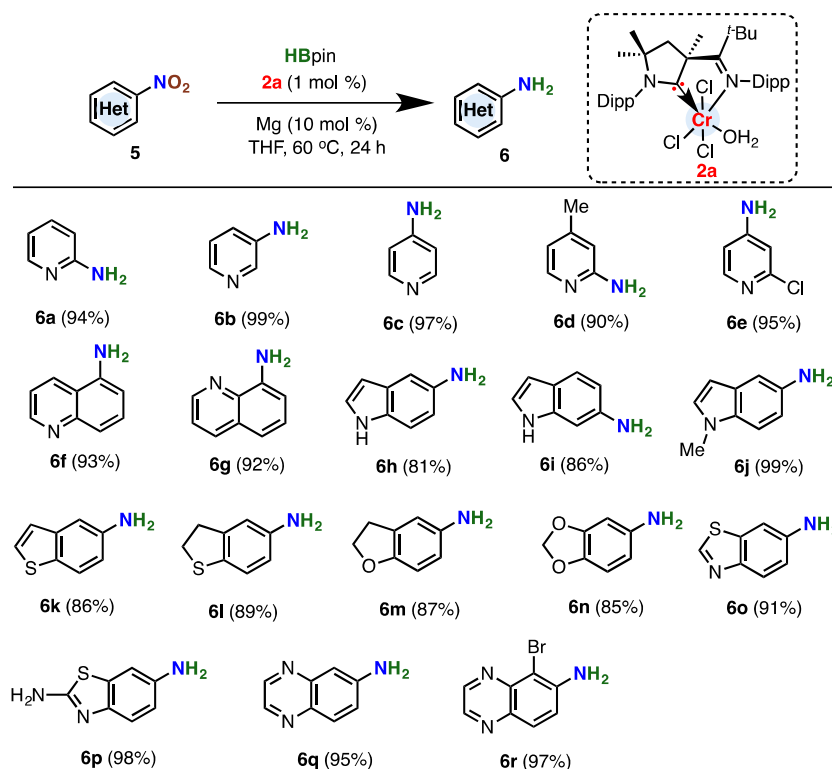
compound **4a** in ~5% yield within the initial 3 h; subsequently, after a further 7.5 h, the reaction takes place rapidly to afford **4a** in 91% yield (see Figure S1). The results indicated that an induction period may be considered for the formation of catalytically active Cr species in the reaction.

We then performed kinetic studies. First, we carried out the reduction of a catalytic amount of **2a** with Mg at 60 °C for 3 h, followed by treatment of the resulting mixture with **3a** and HBpin. The reaction profile suggests, initially, a linear increase in conversion (Figure 2).

To examine the oxidation state of the Cr species after the reduction of CAAC–Cr **2a** by Mg, analysis of Cr 2p by core-level X-ray photoelectron spectroscopy (XPS) was performed, which was fitted with spin–orbital split 2p<sub>1/2</sub> and 2p<sub>3/2</sub> components. The related spectrum showed two sets of XPS peaks, with the 2p<sub>1/2</sub> component appearing at 583.58 eV and the 2p<sub>3/2</sub> component appearing at 574.51 eV for the binding

energies, respectively (Figure S8). These data are in close accordance with those relating to binding energies for Cr(0), indicating that the formation of Cr(0) species by the reduction of **2a** with Mg can be considered.<sup>43</sup>

Using the reactive Cr that was formed in situ by the reduction of **2a** with Mg, the initial reaction rate ( $\Delta[3a]/\Delta t$ ) against the initial concentration of **3a** (in the range 0.025–0.125 M) showed a slope of 0.83 from the logarithm plot and linear fitting of the data, indicating a deviation from the first-order dependence of the initial rate on the concentration of 1-bromo-4-nitrobenzene (Figure 3a). Analogously, the initial reaction rate suggests a positive response to [HBpin], as well as to the CAAC–Cr at low concentration (Figure 3b and c). The logarithmic plot and linear fitting of the data showed a deviation from the first-order dependence of the initial rate on the concentration of HBpin and CAAC–Cr. This indicated

Scheme 3. CAAC–Cr-Catalyzed Deoxygenative Hydroboration of Nitro Heteroarenes for the Synthesis of Heteroaryl Amines<sup>a</sup>

<sup>a</sup>Reactions were conducted on a 0.5 mmol scale. Isolated yields are given.

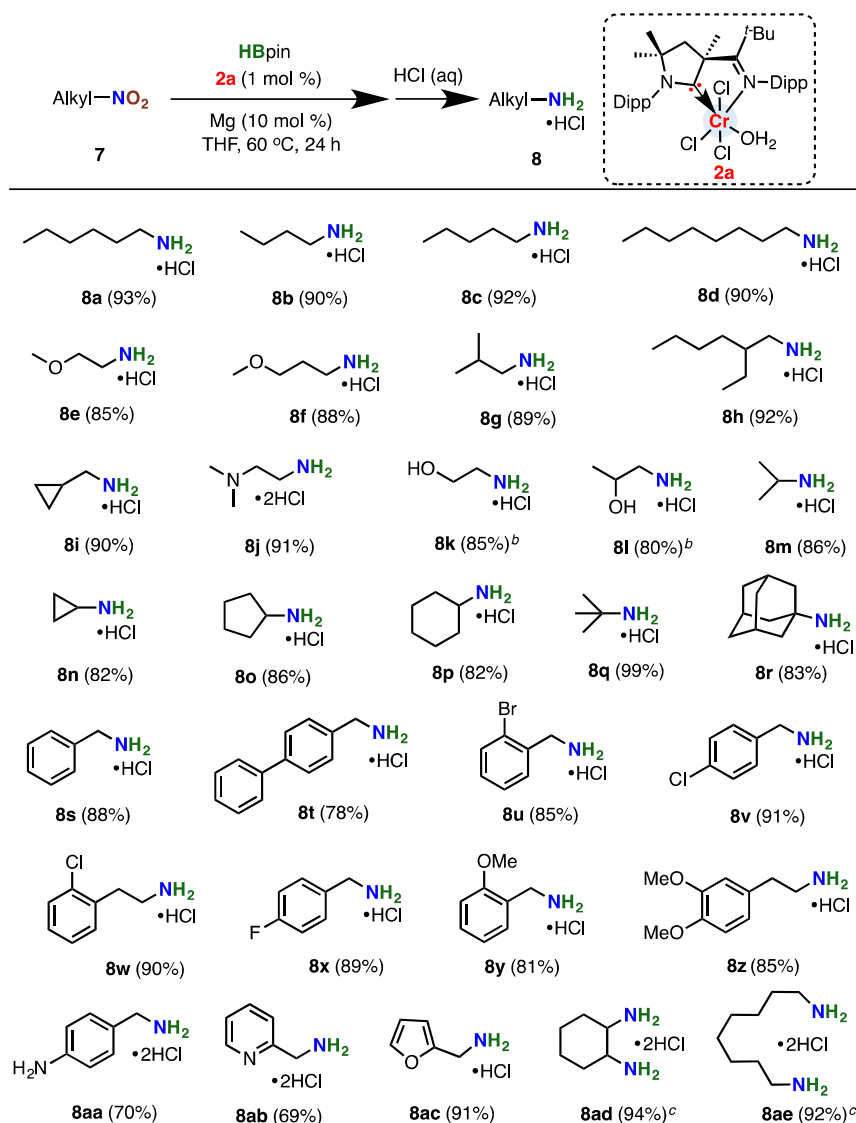
that both pinacolborane and CAAC–Cr are likely involved in the turnover-limiting step of the deoxygenative hydroboration.

The influence of electronic variation of the nitrobenzene component on the deoxygenative hydroboration was then examined from Hammett studies. A linear correlation with Hammett  $\sigma$  constants ( $\rho = +0.74$ ,  $R^2 = 0.95$ ) was observed, and this suggests that the deoxygenative hydroboration in which electron-deficient *para*-nitrobenzenes are used leads to a higher initial reaction rate (Figure 3d). The kinetic experiments of the reaction between nitrobenzene (3e) and HBpin were also carried out at different temperatures. The related Eyring plot in the temperature range 333–353 K revealed the following activation parameters:  $\Delta H^\ddagger = 30.3 \pm 1.7$  kcal mol<sup>-1</sup>,  $\Delta S^\ddagger = 13.6 \pm 4.9$ , and  $\Delta G^\ddagger(298\text{ K}) = 29.3$  kcal mol<sup>-1</sup> (Figure 4).

To understand further the mechanism of CAAC–Cr-catalyzed deoxygenative hydroboration, density functional theory (DFT) modeling of the catalytic cycle was carried out using nitrobenzene at the SMD-B3LYP-D3(BJ)/def2-TZVP//B3LYP-D3(BJ)/def2-SVP level of theory (Figure 5). Besides in 2a, with a quartet ground state, all reaction intermediates depicted in Figure 5a are in a quintet ground state (Table S12). CAACs with low-lying LUMO levels at the carbene center have exhibited superiority in terms of stabilization of paramagnetic low-valent transition metal species.<sup>51</sup> We noted that the CAAC–Cr complex 2a is incapable of catalyzing the deoxygenation of nitrobenzene without Mg, and kinetic observations indicated that the initial reaction rate is slow. On the basis of these and the results of XPS analysis, the reaction commences with the formation of reactive low-valent Cr(0) species that may be considered.<sup>43</sup> Indeed, the reduction of 2a (28.4 kcal mol<sup>-1</sup>) with Mg afforded IN1 (0.0 kcal mol<sup>-1</sup>) in an exergonic manner (Figure 5a). As a nitro compound can

serve as a neutral ligand to bind to metals, the approach of PhNO<sub>2</sub> toward IN1 leads to ligand exchange at Cr to afford complex IN2 (−56.2 kcal mol<sup>-1</sup>).

The catalytic cycle comprises four major processes: two consecutive deoxygenations, and the reduction and recycling of the catalyst (Figure 5a). Given that PhNO is a suitable precursor, and that it reacts smoothly with HBpin to afford aniline 4e (74% yield) at room temperature, by CAAC–Cr catalysis, it is possible to envision that the intermediacy of a Cr–PhNO complex is formed upon the first deoxygenation. DFT calculations revealed that this transformation leading to IN9 (−114.6 kcal mol<sup>-1</sup>) involves five basic steps (Figure 5b). The oxygen lone pair of the nitro group in IN2 is able to bind to HBpin to afford a Lewis acid/base adduct IN4 (−56.7 kcal mol<sup>-1</sup>) with enhanced hydride character in a B–H scaffold. Following this,  $\sigma$ -bond metathesis by the transition state of TS2 (−50.2 kcal mol<sup>-1</sup>),<sup>52</sup> involving B–H/Cr–O bond cleavage, takes place and results in IN5 (−53.4 kcal mol<sup>-1</sup>). The Wiberg bond index analysis demonstrated a significant weakening of the N–O(1) bond in IN5 (0.9) relative to that in free PhNO<sub>2</sub> (1.5), which then allows for a facile N–O(1) bond scission in TS3 (−48.4 kcal mol<sup>-1</sup>), to generate a thermodynamically favorable IN6 (−107.3 kcal mol<sup>-1</sup>). Attempts to locate a transition state that corresponds to an O(1)–H(1) bond formation from IN6 were unsuccessful, presumably because of the unmatched charge distribution between the H(1) (−0.18 au) and O(1) (−0.99 au) atoms, indicated by natural population analysis. Interestingly, a relaxed potential energy surface scan for consecutively shortening the distance of O(1) and H(1) atoms from IN6 offered evidence of the noninnocent ligand behavior of CAAC, in which the carbene carbon (C(1)) acts as an H-shuttle.<sup>53,54</sup> This offered an indication of a carbene-assisted H migration, which leads to

Scheme 4. Deoxygenative Hydroboration of Nitro Alkanes for the Synthesis of Aliphatic Amine Derivatives<sup>a</sup>

<sup>a</sup>Reactions were conducted on a 0.5 mmol scale. Isolated yields are given. <sup>b</sup>HBpin (5 equiv). <sup>c</sup>HBpin (8 equiv).

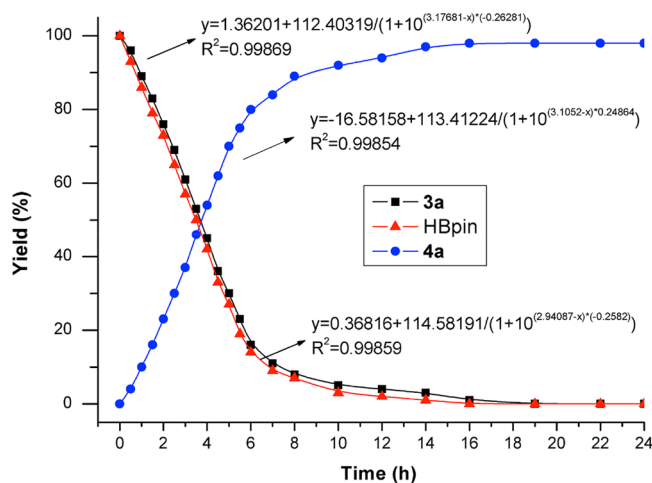


**Figure 2.** Reaction profile for deoxygenative hydroboration of **3a** by using reactive CAAC–Cr that was formed in situ.

polarity reversal of the hydride. Indeed, H(1) can undergo a facile migration to C(1) via **TS4** ( $-101.1 \text{ kcal mol}^{-1}$ ), and this process thus gives rise to an umpolung of the H(1) atom. The H(1) atom appears to be positively charged in **IN7** (0.20 au). Subsequently, the H(1) shift from C(1) to O(1) is achieved in **TSS5** ( $-82.9 \text{ kcal mol}^{-1}$ ) with an activation barrier of  $31.9 \text{ kcal mol}^{-1}$ , followed by elimination of HOBpin to afford the nitrosobenzene-ligated **IN9** ( $-114.6 \text{ kcal mol}^{-1}$ ). It is noteworthy that direct hydroboration of the  $\text{NO}_2$  motif of **IN4** to give **IN5'** was found to be extremely endergonic, by  $64.0 \text{ kcal mol}^{-1}$ , which rules out a Lewis acid-induced hydroboration mechanism (Figure S13).

It has been demonstrated that the non-negligible  $\pi$ -acceptor abilities of singlet carbenes as ligands can influence the outcome of transition-metal catalysis, primarily because of the metal–ligand  $\pi$ -back-donation that tunes the electronic properties of metals.<sup>37</sup> However, on the basis of the H-shuttle behavior observed for CAAC, such carbene ligands may not only be spectator Lewis bases, but also involved in key steps in the Cr-catalyzed deoxygenative hydroboration.<sup>51,53,54</sup> Inspec-

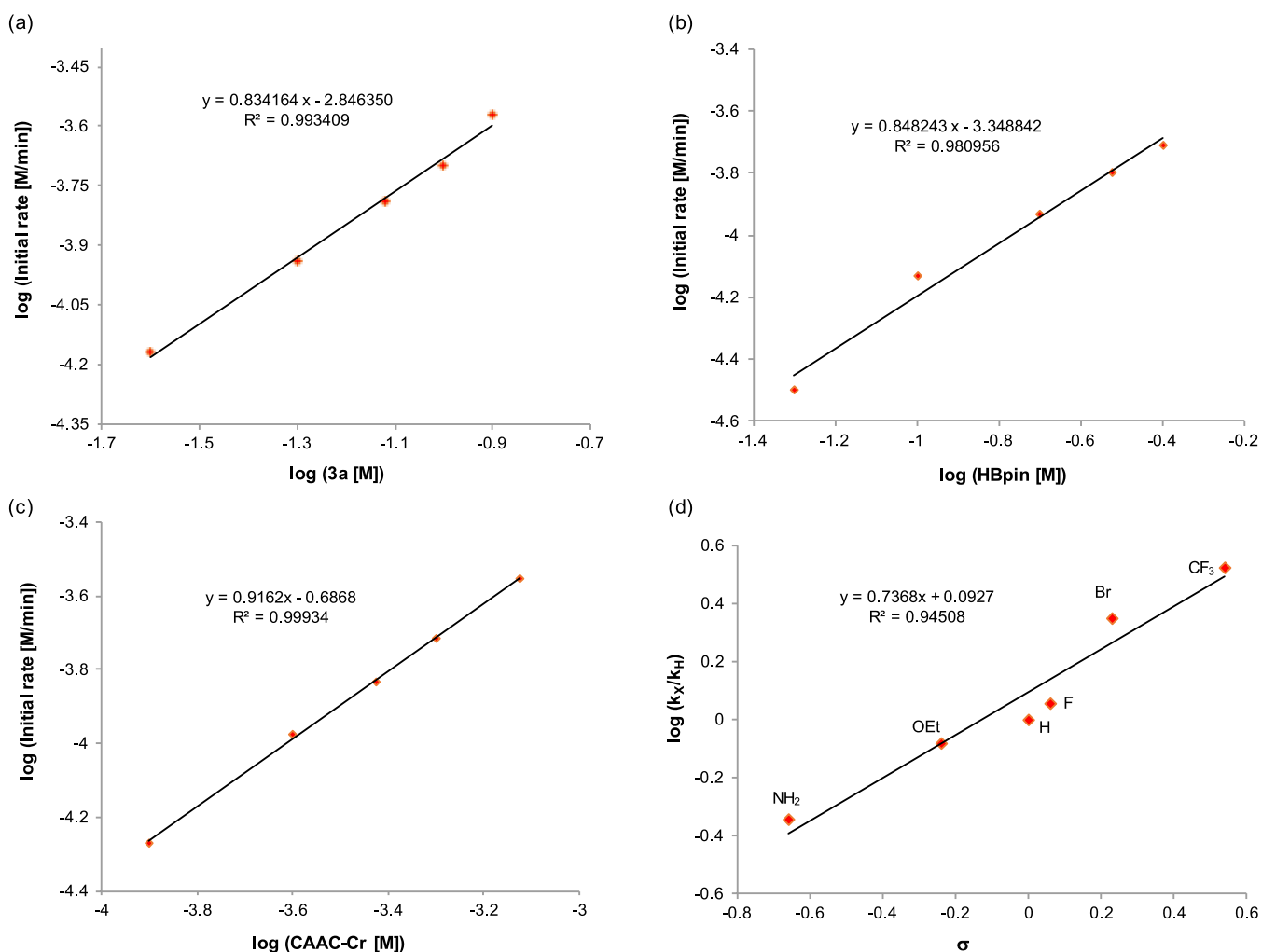


**Figure 3.** Kinetic studies and a Hammett plot. (a) Plot of the initial rate versus the initial concentration of **3a**. (b) Plot of the initial rate versus the concentration of HBpin. (c) Plot of the initial rate versus the concentration of CAAC–Cr. (d) Hammett plot of *para*-substituted nitrobenzenes.

tion of the intrinsic bond orbitals (IBOs),<sup>55</sup> which has been shown to give an exact representation of any Kohn–Sham DFT wave function, reveals that a d-type unpaired electron at Cr highly delocalizes into the formal vacant p-orbital of C(1) in **IN6** (Figure S**6**). This is indicative of the partial radical character of C(1),<sup>38</sup> which may facilitate the H-transfer to **IN7**.

In a similar fashion, the second deoxygenation reaction readily afforded a Cr–nitrene complex **IN16** (−168.0 kcal mol<sup>−1</sup>) and HOBpin, with the highest activation barrier of 15.5 kcal mol<sup>−1</sup> (Figure S10). With the aid of HBpin and HOBpin, the following reduction of **IN16** was also found to not be energy demanding (highest activation barrier 11.6 kcal mol<sup>−1</sup>), affording **IN25** (−196.1 kcal mol<sup>−1</sup>) and O(Bpin)<sub>2</sub> (Figure S11). This was followed by removal of an aniline product from **IN25** in a stepwise manner (highest activation barrier of 25.4 kcal mol<sup>−1</sup>), to complete the catalytic cycle, with regeneration of the nitro-ligated complex **IN2** (Figure S5a). Of note is that the calculated overall energy barrier of 31.9 kcal mol<sup>−1</sup> for the turnover-limiting step of the deoxygenative hydroboration is almost in accordance with the experimental result of the Eyring equation ( $\Delta G^\ddagger(298\text{ K}) = 29.3\text{ kcal mol}^{-1}$ ).

The application of the deoxygenative hydroboration in the preparation of value-added pharmaceuticals was studied. The reaction of nitrobenzene containing pentachloro substituents enabled the selective formation of an aniline-mediated

insecticide of **10** (Scheme 5). Because the hydroxyl group is tolerated by the reaction system, one of the most common pharmaceuticals, paracetamol, which contains a hydroxyl scaffold, was readily accessed (**13**). The treatment of 4-nitrobenzoic acid with HBpin led to the amino-substituted compound **15**, which is one of the key components of folic acid, utilized in the preparation of the anesthetic benzocaine (**16**). The reactions in which (2-nitroethyl)benzene and (3-nitropropyl)benzene were used gave medically interesting compounds (related to hormones, for emotional health and as stimulants) (**18** and **20**). Late-stage functionalization of the resulting amino scaffold, by acylation, resulted in the successful preparation of the drug phenacetin (**23**). Antitubercular agent **25**, which contains three intriguing functionalities (carboxyl, hydroxyl, and amino), is accessible via the deoxygenative hydroboration of commercially available 2-hydroxy-4-nitrobenzoic acid.

### 3. CONCLUSIONS

We developed a CAAC ligand-promoted, pinacolborane-based deoxygenative hydroboration of nitro motifs, with cost-effective chromium catalysis, for application to a diverse range of arenes, heteroarenes, and alkanes. Chemoselectivity in nitro deoxygenative hydroboration over alkynes/olefins, halides, amides, and even *N*-heterocycles of pyridines,

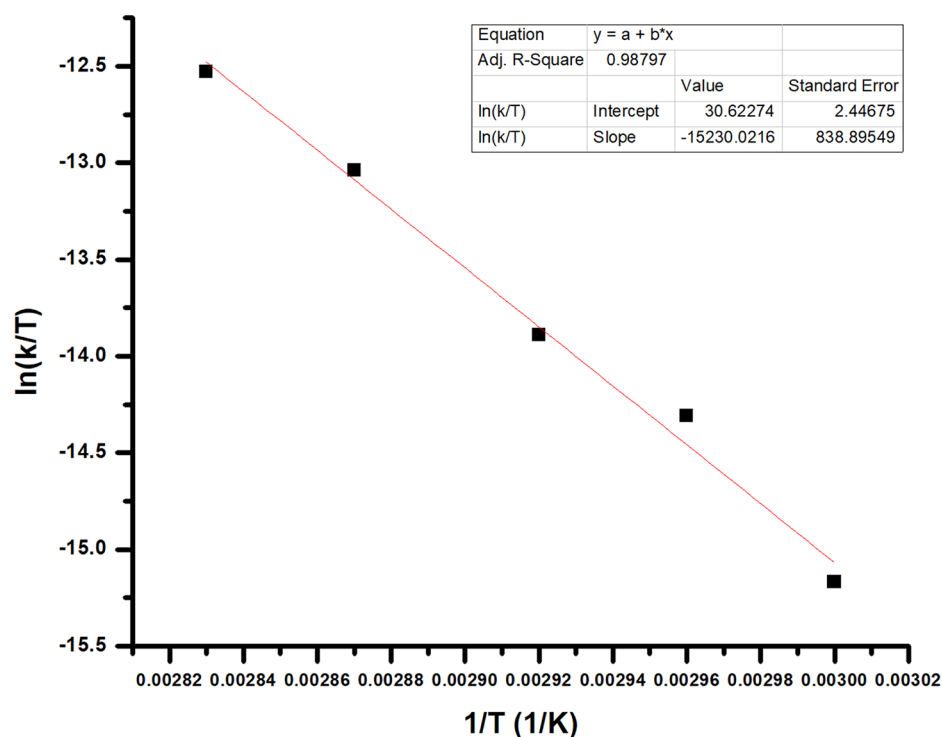


Figure 4. Eyring plot of the deoxygenative hydroboration of nitrobenzene with HBpin.

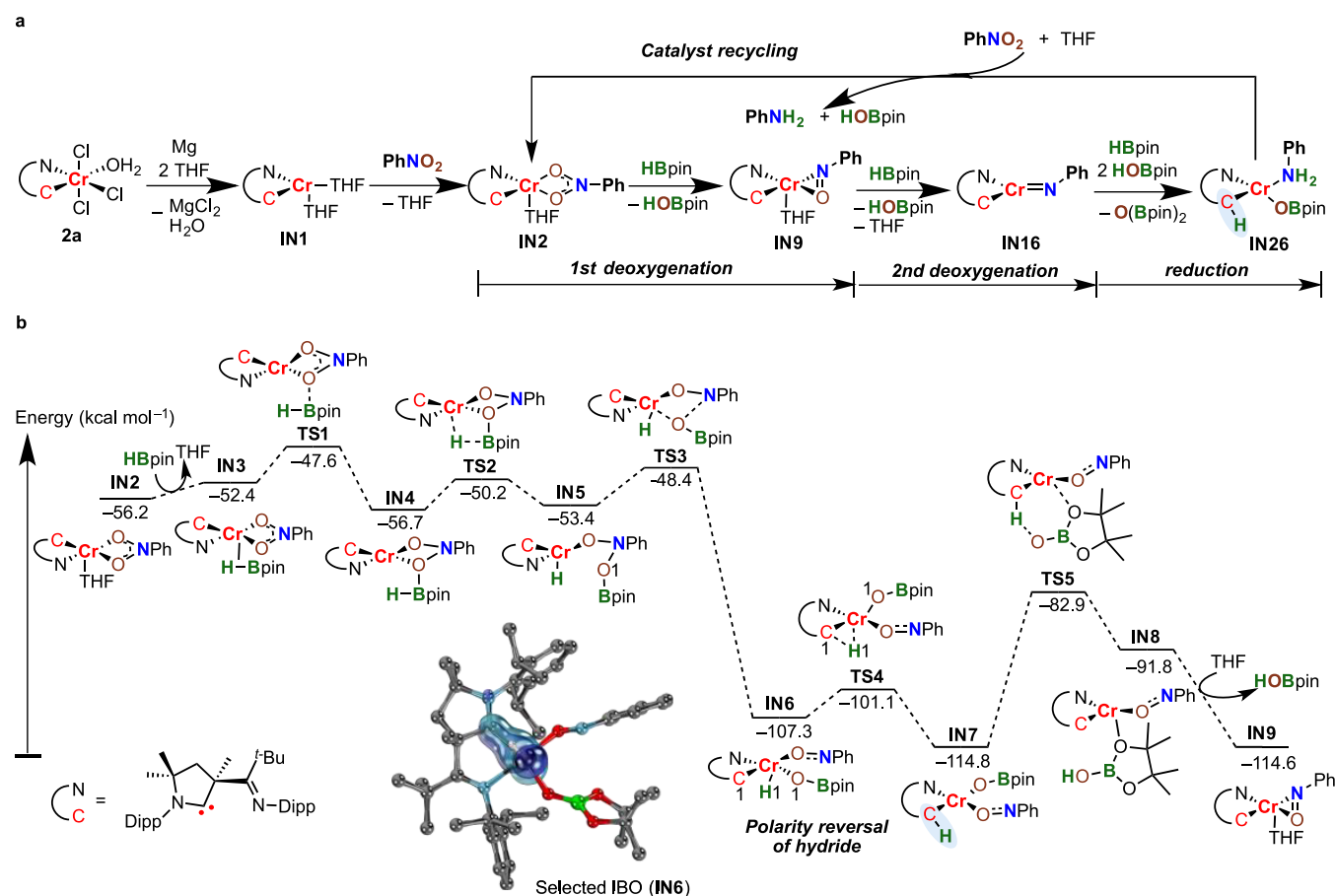
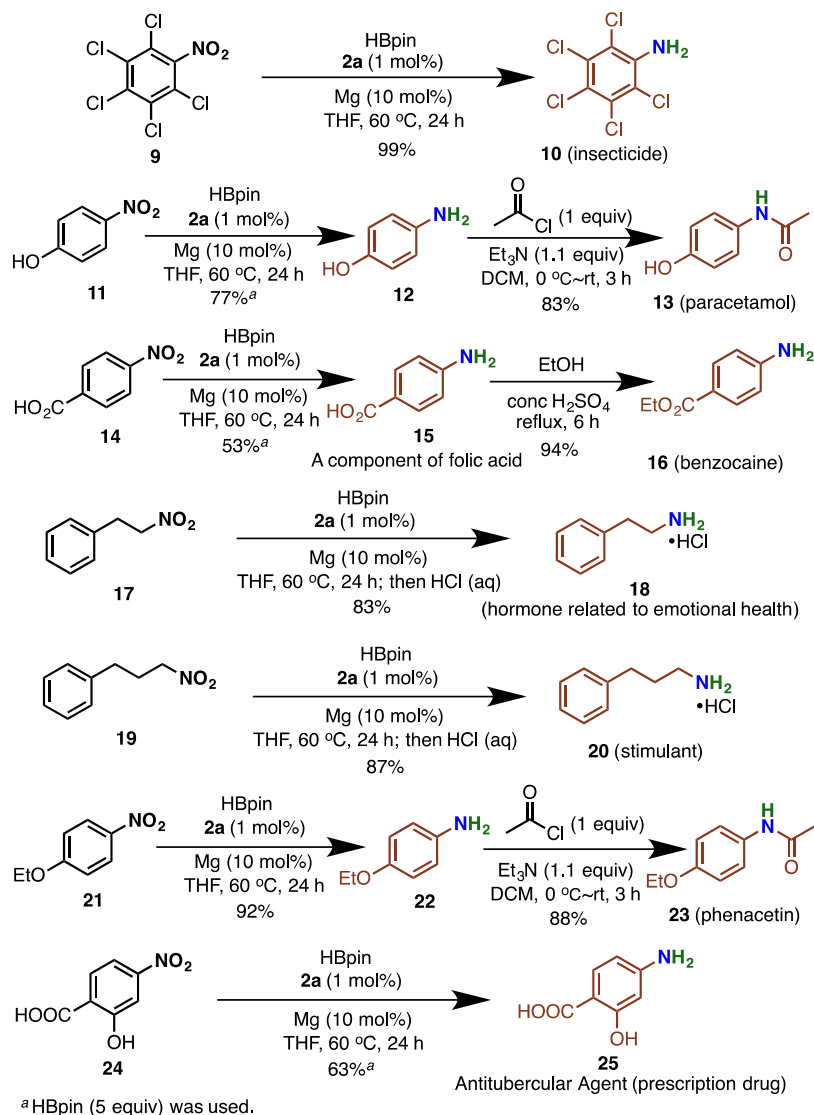


Figure 5. DFT studies carried out to determine the plausible reaction pathway involved in the deoxygenative hydroboration by CAAC–Cr catalysis. (a) Reaction pathway for CAAC–Cr-catalyzed deoxygenation of nitrobenzene identified by DFT calculations. (b) DFT-computed Gibbs free energy profile for the first deoxygenation of nitrobenzene.



## Scheme 5. Application in the Preparation of Pharmaceuticals



quinolines, and indoles, was achieved with particularly high TONs, up to  $1.8 \times 10^6$ . Mechanistic studies indicated that the CAAC ligand serving as a shuttle can be considered to be responsible for the H migration in pinacolborane, by two consecutive deoxygenation and reduction processes, to afford  $\text{NH}_2$  moieties. When using a mild reducing reagent such as HBpin, combined with a highly efficient precatalyst of CAAC–Cr, a safer chemoselective and mild strategy for the deoxygenation of nitro groups is disclosed, highlighting the application of CAACs as ligands and earth-abundant Cr catalysis for molecular construction. Further studies on the isolation of reactive CAAC–Cr intermediates are underway.

#### 4. EXPERIMENTAL SECTION

**Procedure for the Preparation of CAAC–Cr Complex 2a.** A dry Schlenk tube was charged with cyclic iminium salt **1a** (301 mg, 0.5 mmol) and freshly distilled THF (20 mL), through a syringe, under a nitrogen atmosphere, and cooled to  $-78$  °C.  $\text{K}[\text{N}(\text{SiMe}_3)_2]$  (0.5 mmol, 1 M in THF) was added, and the mixture was warmed to room temperature, with stirring, for 0.5 h. The solution was then transferred to a dry Schlenk tube containing  $\text{CrCl}_3$  (79 mg, 0.5 mmol) at  $-78$  °C under atmosphere of nitrogen. The reaction was stirred overnight at room temperature, followed by removal of the solvent

under vacuum. The crude product was purified by recrystallization from dichloromethane and hexane, to afford **2a** as a pale green powder (210 mg, 61% yield). A single crystal of **2a**, suitable for X-ray crystallography, was obtained by recrystallization from a mixed solution of toluene/hexane (1/3).

**General Procedure for the CAAC–Cr-Catalyzed Deoxygenative Hydroboration of Nitroarenes.** THF (2 mL) was added to a dry Schlenk tube containing complex **2a** (3.5 mg, 0.005 mmol), nitroarene (0.5 mmol), HBpin (0.29 mL, 2 mmol), and Mg (1 mg, 0.05 mmol), under a nitrogen atmosphere. The reaction mixture was stirred at 60 °C for 24 h. After the volatiles were removed under a vacuum, the crude product was purified by silica gel chromatography to afford the corresponding aniline product.

#### ■ ASSOCIATED CONTENT

##### Supporting Information

The Supporting Information is available free of charge at <https://pubs.acs.org/doi/10.1021/jacs.0c12318>.

Detailed optimization data; experimental procedures; characterization data of all products, detailed optimized geometries, and computational details and results; and ORTEP drawing of (CAAC)Cr complex **2a** and crystallographic data (PDF)

X-ray crystallographic information for complex **2a** (CIF)

## AUTHOR INFORMATION

### Corresponding Author

Xiaoming Zeng – Key Laboratory of Green Chemistry & Technology, Ministry of Education, College of Chemistry, Sichuan University, Chengdu 610064, China; [orcid.org/0000-0003-0509-1848](https://orcid.org/0000-0003-0509-1848); Email: [zengxiaoming@scu.edu.cn](mailto:zengxiaoming@scu.edu.cn)

### Authors

Lixing Zhao – Key Laboratory of Green Chemistry & Technology, Ministry of Education, College of Chemistry, Sichuan University, Chengdu 610064, China

Chenyang Hu – Shenzhen Grubbs Institute and Department of Chemistry, Southern University of Science and Technology, Shenzhen 518055, China

Xuefeng Cong – Key Laboratory of Green Chemistry & Technology, Ministry of Education, College of Chemistry, Sichuan University, Chengdu 610064, China

Gongda Deng – Key Laboratory of Green Chemistry & Technology, Ministry of Education, College of Chemistry, Sichuan University, Chengdu 610064, China

Liu Leo Liu – Shenzhen Grubbs Institute and Department of Chemistry, Southern University of Science and Technology, Shenzhen 518055, China; [orcid.org/0000-0003-4934-0367](https://orcid.org/0000-0003-4934-0367)

Meiming Luo – Key Laboratory of Green Chemistry & Technology, Ministry of Education, College of Chemistry, Sichuan University, Chengdu 610064, China; [orcid.org/0000-0003-1766-9010](https://orcid.org/0000-0003-1766-9010)

Complete contact information is available at:

<https://pubs.acs.org/10.1021/jacs.0c12318>

### Author Contributions

<sup>§</sup>L.Z. and C.H. contributed equally.

### Notes

The authors declare no competing financial interest.

## ACKNOWLEDGMENTS

We thank the National Natural Science Foundation of China (nos. 21572175, 21871186, and 21971168) and the Fundamental Research Funds for the Central Universities (20826041D4117) for financial support of this research. The theoretical work is supported by the Center for Computational Science and Engineering at SUSTech. L.L.L. gratefully acknowledges the SUSTech start-up fund (Y01216248).

## REFERENCES

- (1) (a) Afanasyev, O. I.; Kuchuk, E.; Usanov, D. L.; Chusov, D. Reductive amination in the synthesis of pharmaceuticals. *Chem. Rev.* **2019**, *119*, 11857–11911.
- (2) (a) Brown, D. G.; Boström, J. Analysis of past and present synthetic methodologies on medicinal chemistry: where have all the new reactions gone? *J. Med. Chem.* **2016**, *59*, 4443–4458. (b) Blakemore, D. C.; Castro, L.; Churcher, I.; Rees, D. C.; Thomas, A. W.; Wilson, D. M.; Wood, A. Organic synthesis provides opportunities to transform drug discovery. *Nat. Chem.* **2018**, *10*, 383–394. (c) Malapit, C. A.; Borrell, M.; Milbauer, M. W.; Brigham, C. E.; Sanford, M. S. Nickel-Catalyzed Decarbonylative Amination of Carboxylic Acid Esters. *J. Am. Chem. Soc.* **2020**, *142*, 5918–5923.
- (3) Formenti, D.; Ferretti, F.; Scharnagl, F. K.; Beller, M. Reduction of nitro compounds using 3d-non-noble metal catalysts. *Chem. Rev.* **2019**, *119*, 2611–2680.

(4) Orlandi, M.; Brenna, D.; Harms, R.; Jost, S.; Benaglia, M. Recent developments in the reduction of aromatic and aliphatic nitro compounds to amines. *Org. Process Res. Dev.* **2018**, *22*, 430–445.

(5) Magano, J.; Dunetz, J. R. Large-scale carbonyl reductions in the pharmaceutical industry. *Org. Process Res. Dev.* **2012**, *16*, 1156–1184.

(6) Roughley, S. D.; Jordan, A. M. The medicinal chemist's toolbox: an Analysis of reactions used in the pursuit of drug candidates. *J. Med. Chem.* **2011**, *54*, 3451–3479.

(7) (a) Goksu, H.; Sert, H.; Kilbas, B.; Sen, F. Recent advances in the reduction of nitro compounds by heterogeneous catalysts. *Curr. Org. Chem.* **2017**, *21*, 794–820. (b) Blaser, H.-U.; Steiner, H.; Studer, M. Selective catalytic hydrogenation of functionalized nitroarenes: an update. *ChemCatChem* **2009**, *1*, 210–221.

(8) Selected examples of homogeneous catalysis: (a) Wienhöfer, G.; Sorribes, I.; Boddien, A.; Westerhaus, F.; Junge, K.; Junge, H.; Llusar, R.; Beller, M. General and Selective Iron-Catalyzed Transfer Hydrogenation of Nitroarenes without Base. *J. Am. Chem. Soc.* **2011**, *133*, 12875–12879. (b) Junge, K.; Wendt, B.; Shaikh, N.; Beller, M. Iron-Catalyzed Selective Reduction of Nitroarenes to Anilines Using Organosilanes. *Chem. Commun.* **2010**, *46*, 1769–1771. (c) Murugesan, K.; Wei, Z.; Chandrashekar, V. G.; Jiao, H.; Beller, M.; Jagadeesh, R. V. General and selective synthesis of primary amines using Ni-based homogeneous catalysts. *Chem. Sci.* **2020**, *11*, 4332–4339.

(9) Selected examples of heterogeneous catalysis: (a) Jagadeesh, R. V.; Surkus, A.-E.; Junge, H.; Pohl, M.-M.; Radnik, J.; Rabeah, J.; Huan, H.; Schünemann, V.; Brückner, A.; Beller, M. Nanoscale Fe<sub>2</sub>O<sub>3</sub>-based catalysts for selective hydrogenation of nitroarenes to anilines. *Science* **2013**, *342*, 1073–1076. (b) Corma, A.; Serna, P. Chemoselective hydrogenation of nitro compounds with supported gold catalysts. *Science* **2006**, *313*, 332–334. (c) Ye, T.-N.; Lu, Y.; Li, J.; Nakao, T.; Yang, H.; Tada, T.; Kitano, M.; Hosono, H. Copper-based intermetallic electride catalyst for chemoselective hydrogenation reactions. *J. Am. Chem. Soc.* **2017**, *139*, 17089–17097. (d) Camacho-Bunquin, J.; Ferrandon, M.; Sohn, H.; Yang, D.; Liu, C.; Ignacio-de Leon, P. A.; Perras, F. A.; Pruski, M.; Stair, P. C.; Delferro, M. Chemoselective Hydrogenation with Supported Organoplatinum(IV) Catalyst on Zn(II)-Modified Silica. *J. Am. Chem. Soc.* **2018**, *140*, 3940–3951. (e) Wang, Y.; Qin, R.; Wang, Y.; Ren, J.; Zhou, W.; Li, L.; Ming, J.; Zhang, W.; Fu, G.; Zheng, N. Chemoselective Hydrogenation of Nitroaromatics at the Nanoscale Iron(III)-OH-Platinum Interface. *Angew. Chem., Int. Ed.* **2020**, *59*, 12736–12740. (f) Boronat, M.; Concepcion', P.; Corma, A.; Gonzal'ez, S.; Illas, F.; Serna, P. A Molecular Mechanism for the Chemoselective Hydrogenation of Substituted Nitroaromatics with Nanoparticles of Gold on TiO<sub>2</sub> Catalysts: A Cooperative Effect between Gold and the Support. *J. Am. Chem. Soc.* **2007**, *129*, 16230–16237.

(10) Selected reviews: (a) Chong, C. C.; Kinjo, R. Catalytic hydroboration of carbonyl derivatives, imines, and carbon dioxide. *ACS Catal.* **2015**, *5*, 3238–3259. (b) Shegavi, M. L.; Bose, S. K. Recent advances in the catalytic hydroboration of carbonyl compounds. *Catal. Sci. Technol.* **2019**, *119*, 2550–2610.

(11) Selected recent examples of hydroboration: (a) Yamamoto, K.; Mohara, Y.; Mutoh, Y.; Saito, S. Ruthenium-catalyzed (Z)-selective hydroboration of terminal alkynes with naphthalene-1,8-diaminoborane. *J. Am. Chem. Soc.* **2019**, *141*, 17042–17047. (b) Feng, Q.; Wu, H.; Li, X.; Song, L.; Chung, L. W.; Wu, Y.-D.; Sun, J. Ru-catalyzed geminal hydroboration of silyl alkynes via a new gem-addition mechanism. *J. Am. Chem. Soc.* **2020**, *142*, 13867–13877. (c) Magre, M.; Paffenholz, E.; Maity, B.; Cavallo, L.; Rueping, M. Regiodivergent hydroborative ring opening of epoxides via selective C–O bond activation. *J. Am. Chem. Soc.* **2020**, *142*, 14286–14294. (d) Kondo, H.; Miyamura, S.; Matsushita, K.; Kato, H.; Kobayashi, C.; Arifin; Itami, K.; Yokogawa, D.; Yamaguchi, J.  $\sigma$ -Bond hydroboration of cyclopropanes. *J. Am. Chem. Soc.* **2020**, *142*, 11306–11313. (e) Bai, X.-Y.; Zhao, W.; Sun, X.; Li, B.-J. Rhodium-catalyzed regiodivergent and enantioselective hydroboration of enamides. *J. Am. Chem. Soc.* **2019**, *141*, 19870–19878. (f) Geri, J.

B.; Szymczak, N. K. A Proton-Switchable Bifunctional Ruthenium Complex That Catalyzes Nitrile Hydroboration. *J. Am. Chem. Soc.* **2015**, *137*, 12808–12814.

(12) Chong, C. C.; Hirao, H.; Kinjo, R. Metal-free  $\sigma$ -bond metathesis in 1,3,2-diazaphospholene-catalyzed hydroboration of carbonyl compounds. *Angew. Chem., Int. Ed.* **2015**, *54*, 190–194.

(13) Wu, D.; Wang, R.; Li, Y.; Ganguly, R.; Hirao, H.; Kinjo, R. Electrostatic catalyst generated from diazadiborinine for carbonyl reduction. *Chem.* **2017**, *3*, 134–151.

(14) Eedugurala, N.; Wang, Z.; Chaudhary, U.; Nelson, N.; Kandel, K.; Kobayashi, T.; Slowing, I. I.; Pruski, M.; Sadow, A. D. Mesoporous silica-supported amidozirconium-catalyzed carbonyl hydroboration. *ACS Catal.* **2015**, *5*, 7399–7414.

(15) Mukherjee, D.; Osseili, H.; Spaniol, T. P.; Okuda, J. Alkali metal hydridotriphenylborates [(L)M][HBPh<sub>3</sub>] (M = Li, Na, K): chemoselective catalysts for carbonyl and CO<sub>2</sub> hydroboration. *J. Am. Chem. Soc.* **2016**, *138*, 10790–10793.

(16) Lebedev, Y.; Polishchuk, I.; Maity, B.; Guerreiro, M. D. V.; Cavallo, L.; Rueping, M. Asymmetric hydroboration of heteroaryl ketones by aluminum catalysis. *J. Am. Chem. Soc.* **2019**, *141*, 19415–19423.

(17) Vasilenko, V.; Blasius, C. K.; Gade, L. H. One-pot sequential kinetic profiling of a highly reactive manganese catalyst for ketone hydroboration: leveraging  $\sigma$ -bond metathesis via alkoxide exchange steps. *J. Am. Chem. Soc.* **2018**, *140*, 9244–9254.

(18) Zhang, G.; Wu, J.; Zheng, S.; Neary, M. C.; Mao, J.; Flores, M.; Trovitch, R. J.; Dub, P. A. Redox-noninnocent ligand-supported vanadium catalysts for the chemoselective reduction of C=X (X = O, N) functionalities. *J. Am. Chem. Soc.* **2019**, *141*, 15230–15239.

(19) Hadlington, T. J.; Hermann, M.; Frenking, G.; Jones, C. Low Coordinate Germanium(II) and Tin(II) Hydride Complexes: Efficient Catalysts for the Hydroboration of Carbonyl Compounds. *J. Am. Chem. Soc.* **2014**, *136*, 3028–3031.

(20) Weidner, V. L.; Barger, C. J.; Delferro, M.; Lohr, T. L.; Marks, T. J. Rapid, mild, and selective ketone and aldehyde hydroboration/reduction mediated by a simple lanthanide catalyst. *ACS Catal.* **2017**, *7*, 1244–1247.

(21) Tamang, S. R.; Findlater, M. Iron catalyzed hydroboration of aldehydes and ketones. *J. Org. Chem.* **2017**, *82*, 12857–12862.

(22) Zhang, G.; Zeng, H.; Wu, J.; Yin, Z.; Zheng, S.; Fettingner, J. C. Highly selective hydroboration of alkenes, ketones and aldehydes catalyzed by a well-defined manganese complex. *Angew. Chem., Int. Ed.* **2016**, *55*, 14369–14372.

(23) Mukherjee, D.; Ellern, A.; Sadow, A. D. Magnesium-catalyzed hydroboration of esters: evidence for a new zwitterionic mechanism. *Chem. Sci.* **2014**, *5*, 959–964.

(24) Barger, C. J.; Motta, A.; Weidner, V. L.; Lohr, T. L.; Marks, T. J. La[N(SiMe<sub>3</sub>)<sub>2</sub>]<sub>3</sub>-catalyzed ester reductions with pinacolborane: scope and mechanism of ester cleavage. *ACS Catal.* **2019**, *9*, 9015–9024.

(25) Erken, C.; Kaithal, A.; Sen, S.; Weyhermüller, T.; Hölscher, M.; Werlé, C.; Leitner, W. Manganese-catalyzed hydroboration of carbon dioxide and other challenging carbonyl groups. *Nat. Commun.* **2018**, *9*, 4521.

(26) Sgro, M. J.; Stephan, D. W. Frustrated lewis pair inspired carbon dioxide reduction by a ruthenium tris(aminophosphine) complex. *Angew. Chem., Int. Ed.* **2012**, *51*, 11343–11345.

(27) Tamang, S. R.; Findlater, M. Cobalt catalyzed reduction of CO<sub>2</sub> via hydroboration. *Dalton Trans.* **2018**, *47*, 8199–8203.

(28) Leong, B.-X.; Lee, J.; Li, Y.; Yang, M.-C.; Siu, C.-K.; Su, M.-D.; So, C.-W. A versatile NHC-parent silyliumylidene cation for catalytic chemo- and regioselective hydroboration. *J. Am. Chem. Soc.* **2019**, *141*, 17629–17636.

(29) Patnaik, S.; Sadow, A. D. Interconverting lanthanum hydride and borohydride catalysts for C=O reduction and C–O bond cleavage. *Angew. Chem., Int. Ed.* **2019**, *58*, 2505–2509.

(30) Lampland, N. L.; Hovey, M.; Mukherjee, D.; Sadow, A. D. Magnesium-catalyzed mild reduction of tertiary and secondary amides to amines. *ACS Catal.* **2015**, *5*, 4219–4226.

(31) Tamang, S. R.; Singh, A.; Bedi, D.; Bazkiaei, A. R.; Warner, A. A.; Glogau, K.; McDonald, C.; Unruh, D. K.; Findlater, M. Polynuclear lanthanide–diketonato clusters for the catalytic hydroboration of carboxamides and esters. *Nat. Catal.* **2020**, *3*, 154–162.

(32) Barger, C. J.; Dicken, R. D.; Weidner, V. L.; Motta, A.; Lohr, T. L.; Marks, T. J. La[N(SiMe<sub>3</sub>)<sub>2</sub>]<sub>3</sub>-catalyzed deoxygenative reduction of amides with pinacolborane. Scope and mechanism. *J. Am. Chem. Soc.* **2020**, *142*, 8019–8028.

(33) Selected reviews of Cr catalysis: (a) Agapie, T. Selective ethylene oligomerization: Recent advances in chromium catalysis and mechanistic investigations. *Coord. Chem. Rev.* **2011**, *255*, 861–880.

(b) Zeng, X.; Cong, X. Chromium-catalyzed transformations with Grignard reagents—new opportunities for cross-coupling reactions. *Org. Chem. Front.* **2015**, *2*, 69–72. (c) Zeng, X. Recent advances in chromium-catalyzed organic transformations. *Synlett* **2020**, *31*, 205–210. (d) Fürstner, A. Carbon–carbon bond formations involving organochromium(III) reagents. *Chem. Rev.* **1999**, *99*, 991–1046.

(34) Selected recent examples of Cr catalysis: (a) Murakami, K.; Ohmiya, H.; Yorimitsu, H.; Oshima, K. Chromium-Catalyzed Arylmagnesiation of Alkynes. *Org. Lett.* **2007**, *9*, 1569–1571.

(b) Yan, J.; Yoshikai, N. Phenanthrene Synthesis via Chromium-Catalyzed Annulation of 2-Biaryl Grignard Reagents and Alkynes. *Org. Lett.* **2017**, *19*, 6630–6633. (c) Liu, P.; Chen, C.; Cong, X.; Tang, J.; Zeng, X. Chromium-catalyzed para-selective formation of quaternary carbon centers by alkylation of benzamide derivatives. *Nat. Commun.* **2018**, *9*, 4637. (d) Steib, A. K.; Kuzmina, O. M.; Fernandez, S.; Flubacher, D.; Knochel, P. Efficient Chromium(II)-Catalyzed Cross-Coupling Reactions between Csp<sup>2</sup> Centers. *J. Am. Chem. Soc.* **2013**, *135*, 15346–15349. (e) Han, B.; Ma, P.; Cong, X.; Chen, H.; Zeng, X. Chromium- and Cobalt-Catalyzed, Regiocontrolled Hydrogenation of Polycyclic Aromatic Hydrocarbons: A Combined Experimental and Theoretical Study. *J. Am. Chem. Soc.* **2019**, *141*, 9018–9026. (f) Yan, J.; Yoshikai, N. Chromium-catalyzed migratory arylmagnesiation of unactivated alkynes. *Org. Chem. Front.* **2017**, *4*, 1972–1975.

(g) Hirscher, N. A.; Sierra, D. P.; Agapie, T. Robust Chromium Precursors for Catalysis: Isolation and Structure of a Single-Component Ethylene Tetramerization Precatalyst. *J. Am. Chem. Soc.* **2019**, *141*, 6022–6029. (h) Li, J.; Ren, Q.; Cheng, X.; Karaghiosoff, K.; Knochel, P. Chromium(II)-Catalyzed Diastereoselective and Chemoselective Csp<sup>2</sup>–Csp<sup>3</sup> Cross-Couplings Using Organomagnesium Reagents. *J. Am. Chem. Soc.* **2019**, *141*, 18127–18135. (i) Yin, J.; Li, J.; Wang, G.-X.; Yin, Z.-B.; Zhang, W.-X.; Xi, Z. Dinitrogen Functionalization Affording Chromium Hydrazido Complex. *J. Am. Chem. Soc.* **2019**, *141*, 4241–4247. (j) Schwarz, J. L.; Schäfers, F.; Tlahuext-Aca, A.; Lückemeier, L.; Glorius, F. Diastereoselective Allylation of Aldehydes by Dual Photoredox and Chromium Catalysis. *J. Am. Chem. Soc.* **2018**, *140*, 12705–12709. (k) Schwarz, J. L.; Kleinmans, R.; Paulisch, T. O.; Glorius, F. 1,2-Amino Alcohols via Cr/Photoredox Dual-Catalyzed Addition of  $\alpha$ -Amino Carbanion Equivalents to Carbonyls. *J. Am. Chem. Soc.* **2020**, *142*, 2168–2174.

(l) Tang, J.; Liu, L. L.; Yang, S.; Cong, X.; Luo, M.; Zeng, X. Chemoselective Cross-Coupling between Two Different and Unactivated C(aryl)–O Bonds Enabled by Chromium Catalysis. *J. Am. Chem. Soc.* **2020**, *142*, 7715–7720. (m) Chen, M.; Doba, T.; Sato, T.; Razumkov, H.; Ilies, L.; Shang, R.; Nakamura, E. Chromium(III)-Catalyzed C(sp<sup>2</sup>)–H Alkynylation, Allylation, and Naphthalenation of Secondary Amides with Trimethylaluminum as Base. *J. Am. Chem. Soc.* **2020**, *142*, 4883–4891.

(35) Selected reviews of NHC-promoted metal catalysis: (a) Zhao, Q.; Meng, G.; Nolan, S. P.; Szostak, M. N-heterocyclic carbene complexes in C–H activation reactions. *Chem. Rev.* **2020**, *120*, 1981–2048. (b) Hopkinson, M. N.; Richter, C.; Schedler, M.; Glorius, F. An overview of N-heterocyclic carbenes. *Nature* **2014**, *510*, 485–496. (c) Diez-González, S.; Marion, N.; Nolan, S. P. N-heterocyclic carbenes in late transition metal catalysis. *Chem. Rev.* **2009**, *109*, 3612–3676.

(36) Lavallo, V.; Canac, Y.; Präsang, C.; Donnadiu, B.; Bertrand, G. Stable cyclic (alkyl)(amino)carbenes as rigid or flexible, bulky, electron-rich ligands for transition-metal catalysts: a quaternary

carbon atom makes the difference. *Angew. Chem., Int. Ed.* **2005**, *44*, 5705–5709.

(37) Soleilhavoup, M.; Bertrand, G. Cyclic (alkyl)(amino)carbenes (CAACs): stable carbenes on the rise. *Acc. Chem. Res.* **2015**, *48*, 256–266.

(38) Roy, S.; Mondal, K. C.; Roesky, H. W. Cyclic alkyl(amino) carbene stabilized complexes with low coordinate metals of enduring nature. *Acc. Chem. Res.* **2016**, *49*, 357–369.

(39) Chu, J.; Munz, D.; Jazzar, R.; Melaimi, M.; Bertrand, G. Synthesis of hemilabile cyclic (alkyl)(amino)carbenes (CAACs) and applications in organometallic chemistry. *J. Am. Chem. Soc.* **2016**, *138*, 7884–7887.

(40) Park, J. H.; Jung, E. H.; Jung, J. W.; Jo, W. H. A fluorinated phenylene unit as a building block for high-performance n-type semiconducting polymer. *Adv. Mater.* **2013**, *25*, 2583–2588.

(41) Jin, J.; Morales-Ramos, A.; Eidam, P.; Mecom, J.; Li, Y.; Brooks, C.; Hilfiker, M.; Zhang, D.; Wang, N.; Shi D. Tseng, P.-S.; Wheless, K.; Budzik, B.; Evans, K.; Jaworski, J.-P.; Jugus, J.; Leon, L.; Wu, C.; Pullen, M.; Karamshih, B.; Rao, P.; Ward, E.; Laping, N.; Evans, C.; Leach, C.; Holt, D.; Su, X.; Morrow, D.; Fries, H.; Thorneloe, K.; Edwards, R. Novel 3-oxazolidinedione-6-aryl-pyridinones as potent, selective, and orally active EP3 receptor antagonists. *ACS Med. Chem. Lett.* **2010**, *1*, 316–320.

(42) Ito, M.; Itazaki, M.; Nakazawa, H. Selective boryl silyl ether formation in the photoreaction of bisboryloxide/boroxine with hydrosilane catalyzed by a transition-metal carbonyl complex. *J. Am. Chem. Soc.* **2014**, *136*, 6183–6186.

(43) Mock, M. T.; Chen, S.; O'Hagan, M.; Rousseau, R.; Dougherty, W. G.; Kassel, W. S.; Bullock, R. M. Dinitrogen reduction by a chromium(0) complex supported by a 16-membered phosphorus macrocycle. *J. Am. Chem. Soc.* **2013**, *135*, 11493–11496.

(44) (a) Fleige, M.; Möbus, J.; vom Stein, T.; Glorius, F.; Stephan, D. W. Lewis acid catalysis: catalytic hydroboration of alkynes initiated by Piers' borane. *Chem. Commun.* **2016**, *52*, 10830–10833.

(b) Greenhalgh, M. D.; Jones, A. S.; Thomas, S. P. Iron-catalysed hydrofunctionalisation of alkenes and alkynes. *ChemCatChem* **2015**, *7*, 190–222.

(45) Das, S.; Addis, D.; Zhou, S.; Junge, K.; Beller, M. Zinc-catalyzed reduction of amides: unprecedented selectivity and functional group tolerance. *J. Am. Chem. Soc.* **2010**, *132*, 1770–1771.

(46) Selected examples: (a) Liu, W.-J.; Tian, K.; Jiang, H. One-pot synthesis of Ni–NiFe<sub>2</sub>O<sub>4</sub>/carbon nanofiber composites from biomass for selective hydrogenation of aromatic nitro compounds. *Green Chem.* **2015**, *17*, 821–826. (b) Yamane, Y.; Liu, X.; Hamasaki, A.; Ishida, T.; Haruta, M.; Yokoyama, T.; Tokunaga, M. One-Pot Synthesis of Indoles and Aniline Derivatives from Nitroarenes under Hydrogenation Condition with Supported Gold Nanoparticles. *Org. Lett.* **2009**, *11*, 5162–5165. (c) Pisiewicz, S.; Formenti, D.; Surkus, A.-E.; Pohl, M.-M.; Radnik, J.; Junge, K.; Topf, C.; Bachmann, S.; Scalone, M.; Beller, M. Synthesis of Nickel Nanoparticles with N-Doped Graphene Shells for Catalytic Reduction Reactions. *ChemCatChem* **2016**, *8*, 129–134.

(47) Dudnik, A. S.; Weidner, V. L.; Motta, A.; Delferro, M.; Marks, T. J. Atom-efficient regioselective 1,2-dearomatization of functionalized pyridines by an earth-abundant organolanthanide catalyst. *Nat. Chem.* **2014**, *6*, 1100.

(48) Rao, B.; Chong, C. C.; Kinjo, R. Metal-free regio- and chemoselective hydroboration of pyridines catalyzed by 1,3,2-diazaphosphenium triflate. *J. Am. Chem. Soc.* **2018**, *140*, 652–656.

(49) Arrowsmith, M.; Hill, M. S.; Hadlington, T.; Kociok-Köhn, G.; Weetman, C. Magnesium-catalyzed hydroboration of pyridines. *Organometallics* **2011**, *30*, 5556–5559.

(50) Fan, X.; Zheng, J.; Li, Z. H.; Wang, H. Organoborane catalyzed regioselective 1,4-hydroboration of pyridines. *J. Am. Chem. Soc.* **2015**, *137*, 4916–4919.

(51) Melaimi, M.; Jazzar, R.; Soleilhavoup, M.; Bertrand, G. Cyclic (alkyl)(amino)carbenes (CAACs): recent developments. *Angew. Chem., Int. Ed.* **2017**, *56*, 10046–10068.

(52) Waterman, R.  $\sigma$ -Bond Metathesis: A 30-Year Retrospective. *Organometallics* **2013**, *32*, 7249–7263.

(53) Frey, G. D.; Donnadiou, B.; Soleilhavoup, M.; Bertrand, G. Synthesis of a Room-Temperature-Stable Dimeric Copper(I) Hydride. *Chem. - Asian J.* **2011**, *6*, 402–405.

(54) Grünwald, A.; Heinemann, F. W.; Munz, D. Oxidative addition of water, alcohols and amines in palladium catalysis. *Angew. Chem., Int. Ed.* **2020**, *59*, 21088–21095.

(55) Knizia, G. Intrinsic atomic orbitals: an unbiased bridge between quantum theory and chemical concepts. *J. Chem. Theory Comput.* **2013**, *9*, 4834–4843.